This document is the Accepted Manuscript version of a Published Work that appeared in final form in ACS Applied Materials and Interfaces, copyright © American Chemical Society after peer review and technical editing by the publisher. To access the final edited and published work see: https://dx.doi.org/10.1021/acsami.8b05751.

Control of the polarization of ferroelectric capacitors by the concurrent action of light and adsorbates

Fanmao Liu,[†] Ignasi Fina,,[†] Guillaume Sauthier,[‡] Florencio Sánchez,[†] Andrew M. Rappe,[§] Josep Fontcuberta[†]*

[†]Institut de Ciència de Materials de Barcelona (ICMAB-CSIC), Campus UAB, Bellaterra 08193, Catalonia, Spain

[‡]Catalan Institute of Nanoscience and Nanotechnology (ICN2), CSIC and The Barcelona Institute of Science and Technology, Campus UAB, Bellaterra 08193, Catalonia, Spain

[§]Department of Chemistry, University of Pennsylvania, Philadelphia, Pennsylvania 19104-6323, United States

KEYWORDS: Ferroelectric, photovoltaic, water, adsorbates, photocatalysis, barium titanate, screening, depolariation field.

*ignasifinamartinez@gmail.com

ABSTRACT. Ferroelectric perovskites hold promise of enhanced photovoltaic efficiency and photocatalytic activity. Consequently, the photoresponse of oxide ferroelectric thin films is an active field of research. In electrode/ferroelectric/electrode devices, internal charge in the ferroelectric, free charge in the electrodes, and buried adsorbates at interfaces combine to screen the ferroelectric polarization and to stabilize the polar state. Under illumination, photo-induced carriers and photo-dissociated adsorbates may disrupt the screening equilibrium, modifying the switchable polarization and altering its expected benefits. Here, we explore the photoresponse of $BaTiO_3$ thin films in a capacitor geometry, focusing on the effects of visible illumination on the remanent polarization. By combining ferroelectric and X-ray photoelectron spectroscopy, we discover that photoreaction of charge-screening H_2O-derived adsorbates at the buried metal-ferroelectric $Pt/BaTiO_3$ interface has an unexpected pivotal role, enabling a substantial modulation (up to 75%) of the switchable remanent polarization by light. These findings illustrate that the synergy between photochemistry and photovoltaic activity at the surface of a ferroelectric material can be exploited to tune photoferroelectric activity.

The non-volatile polarization of ferroelectric materials and their piezoelectric response have been long investigated and exploited in memory elements, sensors and actuators.[1] Photoresponse can arise from depolarization fields resulting from polarization charges and/or from ferroelectrics' non-centrosymmetric character, as discussed in previous works.[2-3] Those ideas are at the root of the renewed interest in the photoresponse of ferroelectrics and the emerging field of photoferroelectrics.[4-11] The typically large band gaps of ferroelectric oxides and their limited photovoltaic efficiency have been challenging bottlenecks for their implementation in photovoltaics. However, in recent times, the observation of larger than band-gap open circuit photo-voltages in ferroelectric thin films[12-15] or photocurrent switchable by electric fields,[16] and

the fresh experimental report of engineered ferroelectric oxides with band gaps in the visible range[17-18] have greatly enhanced the prospects for this class of photovoltaics.

Ferroelectric materials are characterized by the presence of spontaneous polarization (*P*) and concomitant surface charges. Due to energy considerations, typically ferroelectric materials break up into polar domains with different polarization directions. In the case of the prototypical tetragonal phase of $BaTiO_3$ (BTO), domains may form up/down patterns, with the correspondingly positive/negative surface charges, along the tetragonal c-axis direction. However, to stabilize large ferroelectric domains, the surface charge should be properly screened. Screening may be accomplished externally (by charges provided by metallic electrodes, adsorbates, *etc*) or internally (by cationic non stoichiometries, oxygen vacancies, space charge regions, *etc*).[19] The interplay between ferroelectric screening and surface states allows the control of ferroelectric properties, such as Curie temperature or polarization, either by modifying the environment conditions,[20-21] or providing adsorbates (mainly water-related).[22-28] In particular, it is well established that water adsorbates can govern ferroelectric switching dynamics, affecting domain wall morphology and propagation speed.[29-35] By the same token, ferroelectric polarization can determine surface properties providing polarization-sensitive adsorption sites for physisorbed and chemisorbed adsorbates,[36-39] dissociation,[40-41] oxidation/reduction processes,[42-44] and different surface terminations.[38, 45] Under suitable illumination, ferroelectric materials may display radically different ferroelectric properties. Three main mechanisms are at play. First, photoinduced electron-hole pairs within the ferroelectric may provide internal screening, thus reducing the surface potential contrast;[46-47] second, filling pre-existing charge-traps can modify domain pinning and imprint;[48] third bulk photovoltaic effects can drive free carriers to surfaces, enhancing or suppressing polarization.[49]

Overall, detailed knowledge exists on the role of adsorbates and the photoresponse of free ferroelectric surfaces. However, practical photovoltaic devices require the fabrication and use of metal/ferroelectric/metal structures with *capacitor* configuration. In such structures, metallic electrodes and buried adsorbates at metal/ferroelectric interfaces come into play, disturbing screening mechanisms and thus electric field distributions in the devices, whose impact on device photoresponse is largely unknown. In seminal papers, Land and Peercy[50-51] and Dimos and Warren[52-55] reported that under UV irradiation, the polarization loops of some ferroelectric capacitors, made from polycrystalline samples, displayed remarkable changes most notably a dramatic reduction of the polarization and a modification of imprint. Although it was early proposed that the observed effects were related to charge trapping at grain boundaries,[52] this model was challenged by the observation of similar effects in BTO single crystals,[56] suggesting that point bulk defects may play a role. Kholkin[57] also reported a reduction of piezoresponse of PZT films under UV and suggested that a reduction of the depletion layer in the semiconducting PZT, and the concomitant inhomogeneous electric field inside the film, could stimulate the growth of domains of opposite polarity and a reduction of the measured polarization. Gruverman[58] reported the intriguing observation that the polarization loops of $PbTiO_3$ capacitors and $PbTiO_3$ bare films shift oppositely under UV illumination, suggesting a pivotal and distinct role of dielectric layers at ferroelectric surfaces and interfaces on the interaction between photoinduced carriers and polarization charges.

Here we aim to go a step further by addressing the role of adsorbates on the polarization of metal/ferroelectric/metal capacitors *and* on its sensitivity to sub-band gap photon irradiation (3.06 eV). Polarization loops of BTO capacitors were measured using semitransparent Pt electrodes deposited either on fresh or H_2O-exposed BTO surfaces. We found that the remanent polarization

is reduced under illumination, and the effect is more pronounced if the BTO surface has been exposed to H_2O prior to electrode deposition. In an accompanying set of experiments, we have characterized a series of BTO films with electrodes deposited after exposing the samples to ambient conditions. Consistently, it is found that all films display a noticeable reduction of the remanent polarization. X-ray photoelectron spectroscopy shows that the concentration of OH^- adsorbates varies (decreases) with photon illumination and correlates with the observed photosensitivity ΔP_r, suggesting that buried adsorbates at the metal/ferroelectric interface are instrumental in the photoresponse. These findings indicate that embedded adsorbates in tandem with photocarriers play a dominant roles and determine the polarization of ferroelectric.

RESULTS AND DISCUSSION

Experiments were designed to modify the concentration of adsorbed species in a given film and explore the photosensitivity of its polarization. With that purpose, we exposed freshly BTO thin films grown by Pulsed Laser Deposition on $La_{2/3}Sr_{1/3}MnO_3$(LSMO)-buffered (acting as bottom electrode) $SrTiO_3$(001) (STO) substrates to water steam. The *steam treatment* consists of placing the film, at 100 ºC, in a jet of water vapor (800 $cm^3 \cdot min^{-1}$) at atmospheric pressure for 10 hours. After the *steam treatment*, the surfaces of the films were gently dried by a jet of N_2 gas for 1 min to eliminate water residues. After subsequent growth of the Pt electrodes, we recorded the photoresponse of the remanent polarization, and it was compared to that of virgin (un-treated) samples whose electrodes were deposited just after BTO growth.

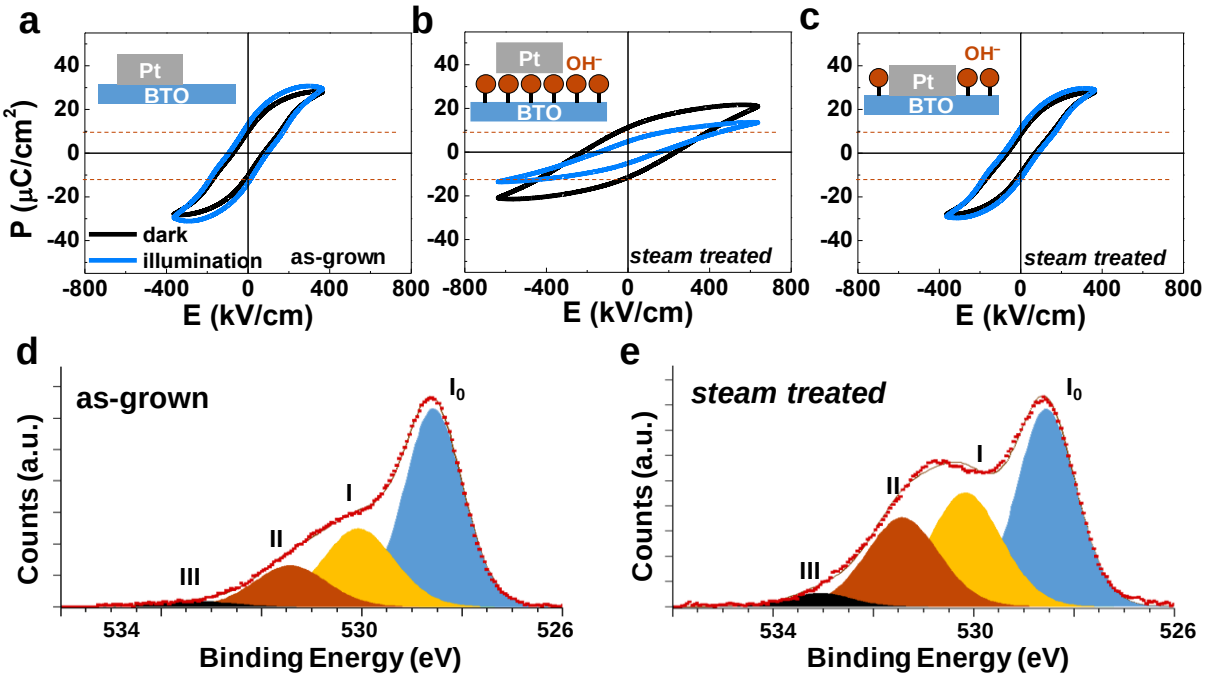

Figure 1. (a) P-E loops of 109.5 nm BTO/LSMO//STO sample, in dark and under illumination, obtained before steam treatment (b) P-E loops in dark and under illumination with top electrodes deposited after 10 h steam treatment. (c) P-E loops in dark and under illumination using electrodes deposited before 10 h steam treatment. Dash lines are guides for the eye to indicate the initial P_r value in dark, and it can be observed that P_r does not significantly change after steam treatment. The insets sketch the Pt/BTO interface; circles (brown) indicates H_2O or OH^- groups attached to the surface. (d, e) O1s XPS spectra of the sample before and after steam treatment.

In Figure 1a, we show the *P-E* loops of a virgin 109.5 nm Pt/BTO/LSMO/STO(001) capacitor. As shown in Figure 1a, the loop recorded under illumination shows only minor variations when compared with the loop recorded in dark. The seemingly small increase of polarization is due to the larger leakage (photovoltaic) current under illumination. After this control experiment, we performed the aforementioned steam treatment, and subsequently deposited new Pt electrodes. In Figure 1b, we show the corresponding *P-E* loops recorded in dark and under illumination.

Comparing the loops in dark before and after *steam treatment*, a small reduction of polarization and a sizeable increase of coercive field are observed, in agreement with the formation of a OH^- layer at the BTO surface (Figure 1b, inset), further supported by dielectric measurements (see Supporting Information Figure S1), and by the small shift of *P-E* loops measured after steam treatment (see Supporting Information Figure S2). More relevant is the observation that the remanent polarization recorded under illumination is reduced compared with that recorded in dark. Interestingly, the *P-E* loops recorded again in the dark and under illumination using the original electrodes after the sample has been steam-treated [Figure 1c] are virtually identical to the fresh contacts of Figure 1a. Therefore, the Pt electrode protects the underneath $BaTiO_3$ surface from additional H_2O adsorption [Figure 1c, inset]. Comparison of data in Figure1a, b and c shows that water-derived adsorbates at the Pt/BTO interface are a key ingredient for the observed photoresponse. Note that, whereas the effect of steam treatment on remanent polarization value measured in dark conditions is small, the effect of steam treatment on the variation of polarization under illumination is large. Thus, the effect of water products at the interface is intriguingly relevant only under illumination conditions.

XPS spectra of the BTO/LSMO//STO film were recorded before [Figure 1d] and after [Figure 1(e)] the *steam treatment*. The spectra are dominated by a main O1s peak (I_0) located at about 528.8 eV, characteristic of lattice O^{2-} (O_L) ions in BTO[59]. Extending towards larger binding energies, a shoulder in the O1s peak is apparent. Previous XPS analyses of BTO[38, 40, 47, 59-61] and other perovskites[62] have shown that this feature results from the contribution of differently bonded oxygen species at the BTO surface. Three components occur at about: (I) 530 eV, (II) 531.5 eV and (III) 533 eV. Peak I (530 eV) has been attributed to protonated lattice oxygen (O_L-H^+)[40, 47] and/or $BaCO_3$[60]. Peak II (531.5 eV) has been attributed to hydroxyl OH^- groups bounded to

surface cations[40, 47] (most likely Ti^{4+} [26, 40]) and peak III (533 eV) is commonly assigned to oxygen hydroxyl groups either bounded to Ba^{2+} ($Ba\text{-}(OH)_2$)[59] or oxygen vacancies (probably present in our films, see Supporting Information Figures S3-4),[40] or physisorbed water H_2O molecules.[62] In brief, components II+III are related to the presence of OH^- or H_2O at the surface, and component I is related to a protonated surface and/or $BaCO_3$. It can not be disregarded the hydrogen incorporation into the $BaTiO_3$ lattice by steam treatment. However, insertion of hydrogen requires rather aggressive (high H_2 pressure, high temperature and long annealing processes)[63-65] or use of hydrogen in chemical precursors.[66-68] None of those conditions are employed here and thus hydrogen insertion should not significantly contribute. This is confirmed by the absence of relevant light absorption at lower photon energy (1.94 eV and 2.38 eV)[69] in our samples. Earlier experiments[64] reported hydrogen-related bands at about 2 eV. Therefore, we exclude a relevant role of hydrogen in the observed effects.

The comparison of data in Figure 1d and Figure 1e indicates that the position of the main I_0 peak (O_L in BTO) is virtually identical before and after the treatment. More interestingly, the high-energy shoulder of the main O1s peak shows an important increase after *steam treatment*. These spectra were analyzed to determine the different (I_0, I, II, and III) contributions and their evolution due to *steam treatment* using suitable deconvolution procedures (see Methods). We used these data as proxy for their relative abundance. Supporting Information Table S1 summarizes the relative areas under the I_0, I, II, and III peaks before and after *steam treatment* and the relative changes of remanent polarization upon illumination (defined as $\Delta P_r = [P_r(\text{dark}) - P_r(\text{illumination})]/P_r(\text{dark})$, where P_r is the remanent polarization). Data in Supporting Information Table S1 show that the major difference in the spectra of Figures 1d,e is related to the II+III components, which significantly increase after *steam treatment*. As II and III O1s peaks are ascribed to the presence

of H_2O-related adsorbates, these results demonstrate that the *steam treatment* promotes their presence, and they are likely responsible for the enhanced ΔP_r photoresponse. If one assumes that adsorbed molecular H_2O is removed during electrode (Pt) deposition, it follows that the enhanced photoresponse after the *steam treatment* is due to the increased presence of chemisorbed OH^- groups at the $BaTiO_3$ surface, underneath the newly-grown Pt electrodes, after treatment. Although the AFM images collected after *steam treatment* show an increased presence of adsorbate-related products, no changes can be seen in the XRD pattern (see Supporting Information Figure S5). We repeated the *steam treatment* experiment in a Pt/BTO/LSMO/DSO and in a thinner Pt/BTO/LSMO/STO capacitor and we obtained similar results (see Supporting Information Figure S6). This points to adsorbate-induced modifications only at the surface.

To confirm the robustness of the fundamental role of buried adsorbates on the photosensitivity of polarization in ferroelectric capacitors, a series of BTO samples of thicknesses 36.5, 73 and 109.5 nm were grown on LSMO-buffered STO and $DyScO_3$ (DSO) substrates and left in ambient conditions for several days before the growth of Pt electrodes. First, we collected XPS spectra of all these BTO films (shown in Supporting Information Figure S7). Focusing on the evolution of the O1s spectra for different films, the relative contribution of each component (I, II, and III and I_0) to the whole O1s spectrum was determined (see Methods in Supporting Information) and used as measure of their relative abundance. The extracted relative fractions of I_0, I, II, III contributions to the O1s peak and the corresponding (I_0 and I) values for Ba3d5/2 are summarized in Supporting Information Table S2. The most important trend is the observed increase of the (II+III) ((OH^-/H_2O)) contribution when increasing film thickness for films grown on both STO and DSO substrates, although more pronounced on DSO. We ascribe the more prominent (II+III) ((OH^-/H_2O)) contribution on thicker films and films grown on DSO to an increase of films'

effective surface area, as revealed by roughness measurements performed by AFM (see Supporting Information Figure S8).

The *P-E* loops of all BTO/LSMO//STO and BTO/LSMO//DSO samples were collected in dark and under illumination (see Supporting Information Figure S9 and the corresponding ΔP_r values included in Supporting Information Table S2). In Figure 2 we plot the relative intensity of II+III (OH^-/H_2O) components, extracted from the XPS spectra, versus the corresponding ΔP_r. Data in Figure 2 show that ΔP_r increases when the relative fraction of (II + III) (OH^-/H_2O) increases. Importantly, this trend holds for BTO films for all thicknesses and both substrates. For completeness, the II+III areas and ΔP_r of the *steam treated* sample of Figure 1 is also included in Figure 2 (stars), showing a fully consistent trend.

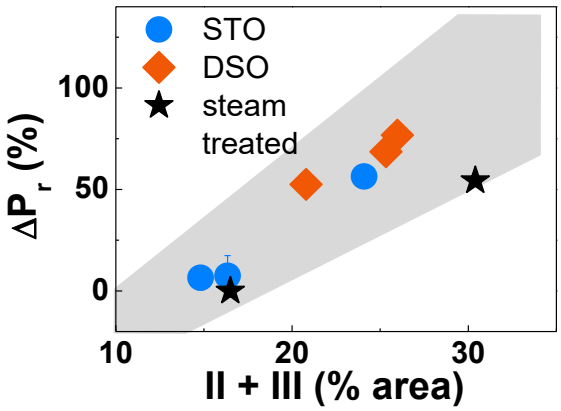

Figure 2. Dependence of the change of remanent polarization with light (ΔP_r) on the relative weights (%) of component II+III (hydroxyl OH^- groups chemisorbed to surface cations and physisorbed water H_2O). The grey background is a guide to the eye. Error bars correspond to the standard deviation of ΔP_r values obtained among 20 measured electrodes in the same sample. When not visible, error bars are smaller than the data point size.

We remind here that XPS spectra give information on the exposed BTO part at the film surface, and ferroelectric characterization is performed using Pt-capped capacitors on the very same film. Therefore, the relative I_0, I, II and III contributions may not represent their actual concentration at the buried BTO surface under the Pt electrode. However, as data in Figure 2 shows that for all samples, including *steam treated* samples, there is a clear connection between the water-related adsorbate contribution to the XPS spectra and ΔP_r, we propose that there is a close link between ΔP_r and the nature and relative abundance of adsorbates.

The hysteresis loops and the XPS data confirm the presence of water and dissociated metal-bonded hydroxyls OH^- and probably O_L-H^+ protons at the buried surface of ferroelectric Pt-covered BTO films. The buried adsorbates modulate the magnitude of the switchable polarization and the polarization variation under illumination (Figures 1 and 2). Therefore, it is crucial to assess any change of adsorbate characteristics under illumination.

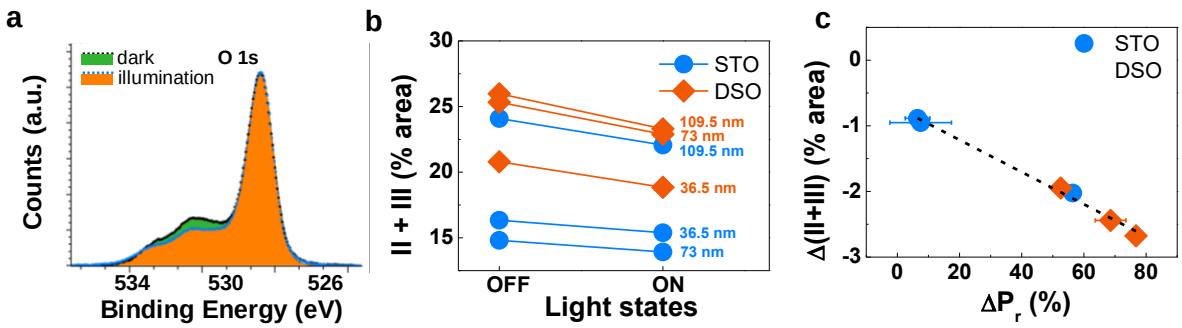

Figure 3. (a) O1s XPS spectrum of BTO (109.5 nm)/LSMO//STO film collected in dark and under illumination. (b) Relative fraction of (II+III) peaks in the O1s XPS spectra of BTO films of different thicknesses and grown on different substrates as indicated. (c) Relative variation under illumination of the (II+III) peaks [Δ(II+III) = [II+III(illumination)]- II+III(dark)] as a function of the ΔP_r values for the whole set of samples.

XPS spectra of all samples were collected in dark and with in-situ illumination, using the same laser (3.06 eV) used in the polarization measurements. In Figure 3a, we show an illustrative XPS spectrum [BTO (109.5 nm/LSMO//STO) recorded in dark (black line) and under illumination (blue line]. It is obvious that the high-energy shoulder (peaks II+III) of O1s is less prominent under illumination. This observation indicates a reduction of the concentration of hydroxyl groups. Spectra of the whole set of samples display similar effects as summarized in Figure 3b, where the relative fractions of (II+III) in dark and under illumination for all samples are plotted. Detailed observation of Figure 3b shows that the relative decrease of the (II+III) fraction in the XPS spectra is more pronounced for samples grown on DSO and for the thicker samples. Recall that the same trend was observed for the phororesponse (ΔP_r) of films on STO and DSO substrates, which was found to be larger in the latter (Figure 2). To emphasize this observation, in Figure 3c, we plot the relative variation of the (II+III) fraction under illumination [$\Delta(II+III) = [II+III(illumination)] - II+III(dark)$] *versus* ΔP_r. These data strongly suggest that there is a correlation between the decrease of the (II+III) fraction in the XPS spectra, related to (OH^-/H_2O) adsorbates, under illumination and the corresponding polarization reduction.

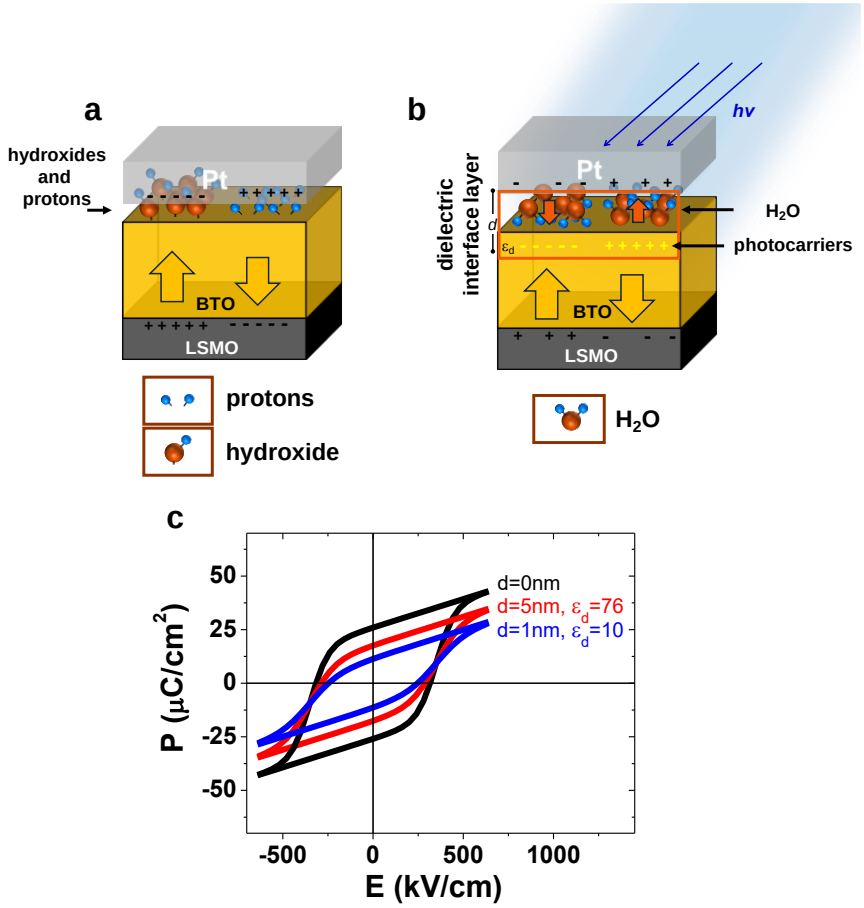

Figure 4. (a) Sketch of the polarization screening in a Pt/$BaTiO_3$ where the metallic electrode has been grown ex-situ after ambient exposure. Chemisorbed OH^- and H^+ radicals, bonded to the surface species, pin ferroelectric polarization. (b) When illuminating the sample through a partially transparent Pt electrode, photocharges screen ferroelectric polarization, reducing the bonding energy of adsorbates and stimulating their oxidation/reduction with the formation of the interface dielectric layer enclosed in red. (c) Calculated polarization loops for a ferroelectric/dielectric bilayer structure having a ferroelectric thickness of 109.5 nm (as in Figure 1) and various (d,ε_d) values as indicated.

Fresh surfaces of BTO films display a minor photo-induced change of remanent polarization ΔP_r indicating that neither external nor internal screening are significantly modified by blue-laser

illumination. The presence of hydroxyl groups (OH^-), probably bonded to Ti^{4+} ions, and O_L-H^+ adsorbates[26] could affect the polarization in coexisting different ways. First in dark conditions, they provide charges contributing to reduce the depolarizing field and pinning a fraction of ferroelectric domains thus reducing the switchable polarization.[70] This effect can be hardly observed in our films by comparing loops of Figures 1a,b measured in dark conditions due to P_r value change after steam treatment is very small. Second, under illumination, photocarriers might contribute to screen the polarization charges, thus making less stable the presence of surface water related products and allowing to their desorption probably forming a thin water layer as described in the next paragraph. The latter effect results in a most pronounced reduction of polarization (this effect is observed while comparing loops of Figure 1b measured in dark and under illumination). The charge redistribution relevant role may occur at both interfaces Pt/adsorbates/BTO and BTO/LSMO. In the first case, charge accumulation at Pt/BTO interface will weaken adsorbates chemisorption energy, making the OH^- and H^+ adsorbates less stable and favoring their oxidation/reduction to forming water molecules, with subsequent reconstruction of the dielectric interface layer at this interface [Figure 4b]. In this case, OH^-/H^+ are instrumental to favor photocarrier accumulation and polarization reduction, in agreement with the effect of water-related adsorbates at the surface on ΔP_r. In the second case, photocarriers will accumulate at the BTO/LSMO interface and may induce the formation of a dielectric layer at the LSMO surface by charge depleting it. However, as this scenario does not require the presence of water-related adsorbates at the Pt/BTO interface, which we have shown to be relevant, we disregard it. In both cases the polarization destabilization can result from the increase of available charges resulting in a decrease of polarization or to its trapping by defects resulting in a polarization internal screening,[3] the fact that the reduction of polarization is persistent after illumination suggests that carriers

trapping may play an important role in the studied system (see Supporting Information Figure S10).

The presence of a newly-formed, photo-induced dielectric interface layer of thickness d and permittivity ε_d at the surface of a ferroelectric film has a strong impact on the polarization loops. It is well-known that the presence of a dielectric interface layer may produce a reduction of polarization. Using the simple model proposed by Tagantsev and Gerra[71] of a dielectric layer of thickness and permittivity (d, ε_d) attached to a ferroelectric film of thickness t and polarization P, polarization loops can be calculated and used to inspect the effects of the dielectric layer. The dependence of $P(E,(d,\ \varepsilon_d))$ for a broad range of (d, ε_d) values can be found in Supporting Information Figure S11. In Figure 4c, we show the *P(E)* loops calculated for a few illustrative values of (d, ε_d) for a BTO film of thickness 109.5 nm as the characterized in Figure 1. Data in this plot clearly illustrate that the dielectric layer reduces the measured polarization. The (d = 1 nm, ε_d= 10) and (d = 5 nm, ε_d= 76) values used in Figure 3c are selected to mimic the observed changed of polarization ($\Delta P_r \approx 60$ %) (Figure 1). It thus follows that the reduction of polarization under illumination can be ascribed to the formation of a dielectric layer of ε_d within (10-76) and a thickness of (1-5) nm. The formation of this dielectric layer is compatible with the observed reduction of the OH^- concentration under illumination, the charge accumulation at the Pt/BTO interface and the relevant role of water related adsorbates presence at the surface and provides a simple description of the photosensitivity of the polarization in Pt/BTO/LSMO heterostructures. Demonstration of the gradual introduction of the added by light dielectric layer can be inferred from the gradual reduction of P_r for increasing illumination time and light power (see Supporting Information Figure S12).

CONCLUSIONS

We have explored the response of the ferroelectric polarization of Pt/BTO/LSMO capacitors upon blue-laser illumination. We have observed that there is a substantial reduction of remanent polarization under illumination, which appears to be directly correlated with the relative concentration of dissociated OH^- and H^+ adsorbates chemisorbed to the buried BTO surface. We argue that whereas adsorbates underneath the top electrodes introduce a dead layer that increases the coercive electric field in dark conditions, these adsorbates under illumination are released. The adsorbates release is ascribed to the fact that they feel less attraction to the $BaTiO_3$ surface because $BaTiO_3$ surface polarization is partially screened by the photoexcited carriers. The released adsorbates generate a dielectric dead layer that produces a decrease of switchable polarization. In-situ XPS measurements have indeed confirmed that the concentration of OH^- is reduced under illumination, suggesting its oxidation and the formation of a dielectric layer that ultimately decreases the measured polarization. More generally, these findings illustrate how the synergy between photochemistry and photovoltaic activity at the surface of a ferroelectric material can be exploited to tune photoferroelectric activity, providing a simple recipe to manipulate it.

METHODS

Samples growth. A series of BTO (001) films of thicknesses 36.5, 73 and 109.5 nm where grown by pulsed laser deposition on $SrTiO_3$(001) (STO) and $DyScO_3$(110) (DSO) substrates buffered with a 30 nm $La_{2/3}Sr_{1/3}MnO_3$ (LSMO) film acting as bottom electrode. Growth details were reported elsewhere.[69, 72] STO and DSO have a cubic structure and produce a nominal compressive mismatch with BTO of 2.20% and 1.23%, respectively. Pt top contacts (20 nm thick, showing around 14% transparency,[73-74] and 60 x 60 μm^2 width) were grown ex-situ by room-temperature

sputtering on as-grown BTO surfaces, using distinct experimental protocols as described in the text.

Ferroelectric characterization. Polarization-electric field (*P-E*) hysteresis loops were measured in the top-top configuration thus cancelling imprint electric fields that could arise from any asymmetry between top and bottom electrodes, and allowing to obtain symmetric *P-E* loops.[69, 75] The *P-E* loops were measured by applying an electric bias on one Pt electrode and grounding an adjacent one, spaced by 15 μm, and either in dark or under illumination with blue laser (3.06 eV, 10 $W \cdot cm^{-2}$) with ≈300 μm diameter spot, large enough to illuminate two adjacent Pt electrodes homogeneously. The measurement frequency, selected following the protocols described elsewhere,[75] was 1kHz in all cases where leakage and other extrinsic contribution are found to be small.

X-ray photoelectron spectroscopy characterization. The surfaces of films were analyzed by X-ray photoelectron spectroscopy (XPS) collected either in dark or under illumination using the same blue laser.

Further experimental details are in Methods included in Supporting Information.

ASSOCIATED CONTENT

The following files are available free of charge.

Detailed methods, raw data extracted from XPS fittings, sketch of the experimental set-up used for the *steam treatment* experiments, and complementary structural, morphological, XPS, dielectric and photoelectric/ferroelectric characterization is included in Supporting Information (PDF).

AUTHOR INFORMATION

Corresponding Author

*E-mail: ignasifinamartinez@gmail.com

Author Contributions

The manuscript was written through contributions of all authors. All authors have given approval to the final version of the manuscript.

ACKNOWLEDGMENT

This work is supported by the Spanish Government (MAT2014-56063-C2-1-R, MAT2017-85232-R and MAT2015-73839-JIN and associated FEDER), and by the Catalan Government (2014 SGR 734). ICMAB-CSIC authors acknowledge financial support from the Spanish Ministry of Economy and Competitiveness, through the "Severo Ochoa" Programme for Centres of Excellence in R&D (SEV- 2015-0496). I. Fina acknowledges Juan de la Cierva – Incorporación postdoctoral fellowship (IJCI-2014-19102) from the Spanish Ministry of Economy and Competitiveness. F. Liu is financially supported by China Scholarship Council (CSC) with No. 201306020016. A.M. Rappe acknowledges support from the Office of Naval Research under grant N00014-17-1-2574. The ICN2 is funded by the CERCA programme / Generalitat de Catalunya. The ICN2 is supported by the Severo Ochoa programme of the Spanish Ministry of Economy, Industry and Competitiveness (MINECO, grant no. SEV-2013-0295).

REFERENCES

1. Setter, N.; Damjanovic, D.; Eng, L.; Fox, G.; Gevorgian, S.; Hong, S.; Kingon, A.; Kohlstedt, H.; Park, N.; Stephenson, G., Ferroelectric thin films: Review of materials, properties, and applications. *J. Appl. Phys.* **2006,** *100*, 051606.

2. Brody, P. S.; Crowne, F., Mechanism for the high voltage photovoltaic effect in ceramic ferroelectrics. *J. Electron. Mater.* **1975,** *4*, 955-971.

3. Fridkin, V. M., *Photoferroelectrics*. Springer-Verlag Berlin Heidelberg: New York, 1979.

4. Huang, H., Solar energy: Ferroelectric photovoltaics. *Nat. Photonics* **2010,** *4*, 134-135.

5. Kreisel, J.; Alexe, M.; Thomas, P., A photoferroelectric material is more than the sum of its parts. *Nat. Mat.* **2012,** *11*, 260-260.

6. Xiao, Z.; Yang, B.; Huang, J., Arising applications of ferroelectric materials in photovoltaic devices. *J. Mater. Chem. A* **2014,** *2*, 6027-6041.

7. Seidel, J.; Eng, L. M., Shedding light on nanoscale ferroelectrics. *Curr. Appl Phys.* **2014,** *14*, 1083-1091.

8. Butler, K. T.; Frost, J. M.; Walsh, A., Ferroelectric materials for solar energy conversion: photoferroics revisited. *Energy Environ. Sci* **2015,** *8*, 838-848.

9. Paillard, C.; Bai, X.; Infante, I. C.; Guennou, M.; Geneste, G.; Alexe, M.; Kreisel, J.; Dkhil, B., Photovoltaics with Ferroelectrics: Current Status and Beyond. *Adv. Mater.* **2016,** *28*, 5153-5168.

10. Lopez-Varo, P.; Bertoluzzi, L.; Bisquert, J.; Alexe, M.; Coll, M.; Huang, J.; Jimenez-Tejada, J. A.; Kirchartz, T.; Nechache, R.; Rosei, F.; Yuan, Y., Physical aspects of ferroelectric semiconductors for photovoltaic solar energy conversion. *Phys. Rep.* **2016,** *653*, 1-40.

11. Young, S. M.; Rappe, A. M., First principles calculation of the shift current photovoltaic effect in ferroelectrics. *Phys. Rev. Lett.* **2012,** *109*, 116601.

12. Yang, S. Y.; Seidel, J.; Byrnes, S. J.; Shafer, P.; Yang, C. H.; Rossell, M. D.; Yu, P.; Chu, Y. H.; Scott, J. F.; Ager, J. W.; Martin, L. W.; Ramesh, R., Above-bandgap voltages from ferroelectric photovoltaic devices. *Nat. Nanotech.* **2010,** *5*, 143-147.

13. Zenkevich, A.; Matveyev, Y.; Maksimova, K.; Gaynutdinov, R.; Tolstikhina, A.; Fridkin, V., Giant bulk photovoltaic effect in thin ferroelectric $BaTiO_3$ films. *Phys. Rev. B* **2014,** *90*, 161409.

14. Alexe, M.; Hesse, D., Tip-enhanced photovoltaic effects in bismuth ferrite. *Nat. Commun.* **2011,** *2*, 256.

15. Spanier, J. E.; Fridkin, V. M.; Rappe, A. M.; Akbashev, A. R.; Polemi, A.; Qi, Y.; Gu, Z.; Young, S. M.; Hawley, C. J.; Imbrenda, D., Power conversion efficiency exceeding the Shockley–Queisser limit in a ferroelectric insulator. *Nat. Photonics* **2016,** *10*, 611-616.

16. Choi, T.; Lee, S.; Choi, Y.; Kiryukhin, V.; Cheong, S.-W., Switchable ferroelectric diode and photovoltaic effect in $BiFeO_3$. *Science* **2009,** *324*, 63-66.

17. Grinberg, I.; West, D. V.; Torres, M.; Gou, G.; Stein, D. M.; Wu, L.; Chen, G.; Gallo, E. M.; Akbashev, A. R.; Davies, P. K., Perovskite oxides for visible-light-absorbing ferroelectric and photovoltaic materials. *Nature* **2013,** *503*, 509-512.

18. Nechache, R.; Harnagea, C.; Li, S.; Cardenas, L.; Huang, W.; Chakrabartty, J.; Rosei, F., Bandgap tuning of multiferroic oxide solar cells. *Nat. Photonics* **2015,** *9*, 61-67.

19. Kalinin, S. V.; Kim, Y.; Fong, D.; Morozovska, A., Surface Screening Mechanisms in Ferroelectric Thin Films and its Effect on Polarization Dynamics and Domain Structures. *arXiv preprint arXiv:1612.08266* **2016**.

20. Fong, D.; Kolpak, A.; Eastman, J.; Streiffer, S.; Fuoss, P.; Stephenson, G.; Thompson, C.; Kim, D.; Choi, K. J.; Eom, C., Stabilization of monodomain polarization in ultrathin $PbTiO_3$ films. *Phys. Rev. Lett.* **2006,** *96*, 127601.

21. Wang, R.; Fong, D.; Jiang, F.; Highland, M.; Fuoss, P.; Thompson, C.; Kolpak, A.; Eastman, J.; Streiffer, S.; Rappe, A., Reversible chemical switching of a ferroelectric film. *Phys. Rev. Lett.* **2009,** *102*, 047601.

22. Shin, J.; Nascimento, V. B.; Geneste, G.; Rundgren, J.; Plummer, E. W.; Dkhil, B.; Kalinin, S. V.; Baddorf, A. P., Atomistic screening mechanism of ferroelectric surfaces: An in situ study of the polar phase in ultrathin $BaTiO_3$ films exposed to H_2O. *Nano Lett.* **2009,** *9*, 3720-3725.

23. Spanier, J. E.; Kolpak, A. M.; Urban, J. J.; Grinberg, I.; Ouyang, L.; Yun, W. S.; Rappe, A. M.; Park, H., Ferroelectric phase transition in individual single-crystalline $BaTiO_3$ nanowires. *Nano Lett.* **2006,** *6*, 735-739.

24. Geneste, G.; Dkhil, B., Adsorption and dissociation of H_2O on in-plane-polarized $BaTiO_3$ (001) surfaces and their relation to ferroelectricity. *Phys. Rev. B* **2009,** *79*, 235420.

25. He, D.; Qiao, L.; Volinsky, A. A.; Bai, Y.; Guo, L., Electric field and surface charge effects on ferroelectric domain dynamics in $BaTiO_3$ single crystal. *Phys. Rev. B* **2011,** *84*, 024101.

26. Koocher, N. Z.; Martirez, J. M. P.; Rappe, A. M., Theoretical Model of Oxidative Adsorption of Water on a Highly Reduced Reconstructed Oxide Surface. *J. Phys. Chem. Lett.* **2014,** *5*, 3408-3414.

27. Lee, H.; Kim, T. H.; Patzner, J. J.; Lu, H.; Lee, J.-W.; Zhou, H.; Chang, W.; Mahanthappa, M. K.; Tsymbal, E. Y.; Gruverman, A., Imprint control of $BaTiO_3$ thin films via chemically induced surface polarization pinning. *Nano Lett.* **2016,** *16*, 2400–2406.

28. Qi, Y.; Martirez, J.; Saidi, W. A.; Urban, J.; Yun, W.; Spanier, J.; Rappe, A., Modified Schottky emission to explain thickness dependence and slow depolarization in $BaTiO_3$ nanowires. *Phys. Rev. B* **2015,** *91*, 245431.

29. Shur, V. Y.; Ievlev, A.; Nikolaeva, E.; Shishkin, E.; Neradovskiy, M., Influence of adsorbed surface layer on domain growth in the field produced by conductive tip of scanning probe microscope in lithium niobate. *J. Appl. Phys.* **2011,** *110*, 052017.

30. Ievlev, A. V.; Morozovska, A. N.; Shur, V. Y.; Kalinin, S. V., Humidity effects on tip-induced polarization switching in lithium niobate. *Appl. Phys. Lett.* **2014,** *104*, 092908.

31. Blaser, C.; Paruch, P., Subcritical switching dynamics and humidity effects in nanoscale studies of domain growth in ferroelectric thin films. *New J. Phys.* **2015,** *17*, 013002.

32. Dahan, D.; Molotskii, M.; Rosenman, G.; Rosenwaks, Y., Ferroelectric domain inversion: The role of humidity. *Appl. Phys. Lett.* **2006,** *89*, 152902.

33. Rodriguez, B. J.; Jesse, S.; Baddorf, A. P.; Kim, S.-H.; Kalinin, S. V., Controlling polarization dynamics in a liquid environment: From localized to macroscopic switching in ferroelectrics. *Phys. Rev. Lett.* **2007,** *98*, 247603.

34. Kalinin, S. V.; Bonnell, D. A., Screening phenomena on oxide surfaces and its implications for local electrostatic and transport measurements. *Nano Lett.* **2004,** *4*, 555-560.

35. Ievlev, A.; Jesse, S.; Morozovska, A.; Strelcov, E.; Eliseev, E.; Pershin, Y.; Kumar, A.; Shur, V. Y.; Kalinin, S., Intermittency, quasiperiodicity and chaos in probe-induced ferroelectric domain switching. *Nat. Phys.* **2014,** *10*, 59-66.

36. Li, D.; Zhao, M.; Garra, J.; Kolpak, A.; Rappe, A.; Bonnell, D.; Vohs, J., Direct in situ determination of the polarization dependence of physisorption on ferroelectric surfaces. *Nat. Mat.* **2008,** *7*, 473-477.

37. Garra, J.; Vohs, J.; Bonnell, D., The effect of ferroelectric polarization on the interaction of water and methanol with the surface of $LiNbO_3$ (0001). *Surf. Sci.* **2009,** *603*, 1106-1114.

38. Saidi, W. A.; Martirez, J. M. P.; Rappe, A. M., Strong reciprocal interaction between polarization and surface stoichiometry in oxide ferroelectrics. *Nano Lett.* **2014,** *14*, 6711-6717.

39. Cordero-Edwards, K.; Rodríguez, L.; Calo, A.; Esplandiu, M. J.; Pérez-Dieste, V.; Escudero, C.; Domingo, N.; Verdaguer, A., Water Affinity and Surface Charging at the z-Cut and y-Cut $LiNbO_3$ Surfaces: An Ambient Pressure X-ray Photoelectron Spectroscopy Study. *J. Phys. Chem. C* **2016,** *120*, 24048-24055.

40. Wang, J.; Gaillard, F.; Pancotti, A.; Gautier, B.; Niu, G.; Vilquin, B.; Pillard, V.; Rodrigues, G.; Barrett, N., Chemistry and atomic distortion at the surface of an epitaxial $BaTiO_3$ thin film after dissociative adsorption of water. *J. Phys. Chem. C* **2012,** *116*, 21802-21809.

41. Zhao, M. H.; Bonnell, D. A.; Vohs, J. M., Effect of ferroelectric polarization on the adsorption and reaction of ethanol on $BaTiO_3$. *Surf. Sci.* **2008,** *602*, 2849-2855.

42. Giocondi, J.; Rohrer, G., Spatial separation of photochemical oxidation and reduction reactions on the surface of ferroelectric $BaTiO_3$. *J. Phys. Chem. B* **2001,** *105*, 8275-8277.

43. Burbure, N. V.; Salvador, P. A.; Rohrer, G. S., Photochemical reactivity of titania films on $BaTiO_3$ substrates: origin of spatial selectivity. *Chem. Mater.* **2010,** *22*, 5823-5830.

44. Cui, Y.; Briscoe, J.; Dunn, S., Effect of Ferroelectricity on Solar-Light-Driven Photocatalytic Activity of $BaTiO_3$ Influence on the Carrier Separation and Stern Layer Formation. *Chem. Mater.* **2013,** *25*, 4215-4223.

45. Levchenko, S. V.; Rappe, A. M., Influence of ferroelectric polarization on the equilibrium stoichiometry of lithium niobate (0001) surfaces. *Phys. Rev. Lett.* **2008,** *100*, 256101.

46. Shao, R.; Nikiforov, M. P.; Bonnell, D. A., Photoinduced charge dynamics on $BaTiO_3$ (001) surface characterized by scanning probe microscopy. *Appl. Phys. Lett.* **2006,** *89*, 112904.

47. Wang, J.; Vilquin, B.; Barrett, N., Screening of ferroelectric domains on $BaTiO_3$(001) surface by ultraviolet photo-induced charge and dissociative water adsorption. *Appl. Phys. Lett.* **2012,** *101*, 092902.

48. Sones, C.; Muir, A.; Ying, Y.; Mailis, S.; Eason, R.; Jungk, T.; Hoffmann, A.; Soergel, E., Precision nanoscale domain engineering of lithium niobate via UV laser induced inhibition of poling. *Appl. Phys. Lett.* **2008,** *92*, 072905.

49. Daranciang, D.; Highland, M. J.; Wen, H.; Young, S. M.; Brandt, N. C.; Hwang, H. Y.; Vattilana, M.; Nicoul, M.; Quirin, F.; Goodfellow, J., Ultrafast photovoltaic response in ferroelectric nanolayers. *Phys. Rev. Lett.* **2012,** *108*, 087601.

50. Land, C.; Peercy, P., A review of the effects of ion implantation on the photoferroelectric properties of PLZT ceramics. *Ferroelectrics* **1982,** *45*, 25-43.

51. Land, C. E.; Peercy, P., Photoferroelectric effects in PLZT ceramics. *Ferroelectrics* **1978,** *22*, 677-679.

52. Dimos, D.; Warren, W. L.; Sinclair, M. B.; Tuttle, B. A.; Schwartz, R. W., Photoinduced hysteresis changes and optical storage in (Pb,La)(Zr,Ti)O_3 thin films and ceramics. *J. Appl. Phys.* **1994,** *76*, 4305-4315.

53. Dimos, D.; Potter, B. G.; Sinclair, M. B.; Tuttle, B. A.; Warren, W. L., Photo-induced and electrooptic properties of (Pb,La)(Zr,Ti)O_3 films for optical memories. *Integr. Ferroelectr.* **1994,** *5*, 47-58.

54. Warren, W. L.; Dimos, D., Photo-assisted switching and trapping in $BaTiO_3$ and Pb(Zr, Ti)O_3 ferroelectrics. *J. Non-Cryst. Solids* **1995,** *187*, 448-452.

55. Warren, W. L.; Dimos, D.; Tuttle, B. A.; Pike, G. E.; Schwartz, R. W.; Clews, P. J.; McIntyre, D. C., Polarization suppression in Pb(Zr,Ti)O_3 thin films. *J. Appl. Phys.* **1995,** *77*, 6695-6702.

56. Warren, W.; Dimos, D., Photoinduced hysteresis changes and charge trapping in $BaTiO_3$ dielectrics. *Appl. Phys. Lett.* **1994,** *64*, 866-868.

57. Kholkin, A. L.; Iakovlev, S. O.; Baptista, J. L., Direct effect of illumination on ferroelectric properties of lead zirconate titanate thin films. *Appl. Phys. Lett.* **2001,** *79*, 2055-2057.

58. Gruverman, A.; Rodriguez, B. J.; Nemanich, R.; Kingon, A., Nanoscale observation of photoinduced domain pinning and investigation of imprint behavior in ferroelectric thin films. *J. Appl. Phys.* **2002,** *92*, 2734-2739.

59. Baniecki, J.; Ishii, M.; Shioga, T.; Kurihara, K.; Miyahara, S., Surface core-level shifts of strontium observed in photoemission of barium strontium titanate thin films. *Appl. Phys. Lett.* **2006,** *89*, 162908.

60. Miot, C.; Husson, E.; Proust, C.; Erre, R.; Coutures, J., Residual carbon evolution in $BaTiO_3$ ceramics studied by XPS after ion etching. *J. Eur. Ceram. Soc.* **1998,** *18*, 339-343.

61. Ayouchi, R.; Martin, F.; Ramos-Barrado, J.; Leinen, D., Compositional, structural and electrical characterization of barium titanate thin films prepared on fused silica and Si (111) by spray pyrolysis. *Surf. Interface Anal.* **2000,** *30*, 565-569.

62. Brown, K. A.; He, S.; Eichelsdoerfer, D. J.; Huang, M.; Levy, I.; Lee, H.; Ryu, S.; Irvin, P.; Mendez-Arroyo, J.; Eom, C.-B., Giant conductivity switching of $LaAlO_3/SrTiO_3$ heterointerfaces governed by surface protonation. *Nat. Commun.* **2016,** *7*, 10681

63. Waser, R., Solubility of hydrogen defects in doped and undoped $BaTiO_3$. *J. Am. Ceram. Soc.* **1988,** *71*, 58-63.

64. Chang, J.; Chinjen, C.; Tsou, R.; Huang, C.; Sun, C.; Chang, M., Photorefractive effect in hydrogen-reduced $BaTiO_3$. *Opt. Commun.* **1997,** *138*, 101-104.

65. Alvine, K. J.; Tyagi, M.; Brown, C. M.; Udovic, T. J.; Jenkins, T.; Pitman, S. G., Hydrogen species motion in piezoelectrics: A quasi-elastic neutron scattering study. *J. Appl. Phys.* **2012,** *111*, 053505.

66. Kobayashi, Y.; Hernandez, O. J.; Sakaguchi, T.; Yajima, T.; Roisnel, T.; Tsujimoto, Y.; Morita, M.; Noda, Y.; Mogami, Y.; Kitada, A., An oxyhydride of $BaTiO_3$ exhibiting hydride exchange and electronic conductivity. *Nat. Mat.* **2012,** *11*, 507.

67. Bouilly, G.; Yajima, T.; Terashima, T.; Yoshimune, W.; Nakano, K.; Tassel, C. d.; Kususe, Y.; Fujita, K.; Tanaka, K.; Yamamoto, T., Electrical properties of epitaxial thin films of oxyhydrides $ATiO_{3-x}H_x$ (A= Ba and Sr). *Chem. Mater.* **2015,** *27*, 6354-6359.

68. Ito, T.; Koda, A.; Shimomura, K.; Higemoto, W.; Matsuzaki, T.; Kobayashi, Y.; Kageyama, H., Excited configurations of hydrogen in the $BaTiO_{3-x}H_x$ perovskite lattice associated with hydrogen exchange and transport. *Phys. Rev. B* **2017,** *95*, 020301.

69. Liu, F.; Fina, I.; Bertacco, R.; Fontcuberta, J., Unravelling and controlling hidden imprint fields in ferroelectric capacitors. *Sci. Rep.* **2016,** *6*, 2835.

70. Kim, S.; Sinai, O.; Lee, C.-W.; Rappe, A. M., Controlling oxide surface dipole and reactivity with intrinsic nonstoichiometric epitaxial reconstructions. *Phys. Rev. B* **2015,** *92*, 235431.

71. Tagantsev, A.; Gerra, G., Interface-induced phenomena in polarization response of ferroelectric thin films. *J. Appl. Phys.* **2006,** *100*, 051607.

72. Liu, F.; Fina, I.; Gutiérrez, D.; Radaelli, G.; Bertacco, R.; Fontcuberta, J., Selecting Steady and Transient Photocurrent Response in $BaTiO_3$ Films. *Adv. Electron. Mater.* **2015,** *1*, 1500171.

73. Windt, D. L.; Cash Jr, W. C.; Scott, M.; Arendt, P.; Newnam, B.; Fisher, R.; Swartzlander, A., Optical constants for thin films of Ti, Zr, Nb, Mo, Ru, Rh, Pd, Ag, Hf, Ta, W, Re, Ir, Os, Pt, and Au from 24 A to 1216 A. *Appl. Opt.* **1988,** *27*, 246-278.

74. Werner, W. S.; Glantschnig, K.; Ambrosch-Draxl, C., Optical constants and inelastic electron-scattering data for 17 elemental metals. *J. Phys. Chem. Ref. Data* **2009,** *38*, 1013-1092.

75. Fina, I.; Fàbrega, L.; Langenberg, E.; Martí, X.; Sánchez, F.; Varela, M.; Fontcuberta, J., Nonferroelectric contributions to the hysteresis cycles in manganite thin films: A comparative study of measurement techniques. *J. Appl. Phys.* **2011,** *109*, 074105.

TABLE OF CONTENTS GRAPHIC